CONSTANT ENVELOPE OFDM PHASE MODULATION: SPECTRAL CONTAINMENT, SIGNAL SPACE PROPERTIES AND PERFORMANCE

Steve C. Thompson*, Ahsen U. Ahmed†*, John G. Proakis*, James R. Zeidler*
*with the Center for Wireless Communications
University of California, San Diego
La Jolla, CA 92093-0407
†with SPAWAR Systems Center, San Diego

ABSTRACT

A class of constant envelope OFDM phase modulated (OFDM-PM) signals is studied. The motivation behind OFDM-PM is to alleviate the high peak-to-average power ratio of conventional OFDM systems. Power density spectrum plots and fractional out-of-band power curves are given. For small modulation indices, the OFDM-PM signals are shown to be more spectrally contained than conventional OFDM. The signal space is studied by considering the correlation properties of the OFDM-PM signals. A performance bound on the optimum OFDM-PM receiver is compared to simulation results. Also, a sub-optimum phase demodulator receiver is analyzed and an AWGN performance approximation is compared to simulation results. It is shown that for a small modulation index and high signal-to-noise ratio, the sub-optimum receiver performs close to the optimum receiver.

INTRODUCTION

It is well known that the high peak-to-average power ratio (PAPR) of orthogonal frequency division multiplexing (OFDM) is a considerable drawback [1], [2]. Typically, power backoff is required for linear amplification which reduces transmitter efficiency [3]. Without sufficient back-off, intermodulation distortion causes both a reduction in spectral efficiency due to out-of-band spectral growth and a loss in performance due to in-band distortion [4].

Many PAPR reduction techniques have been studied [5], [6]. In general, reduction schemes trade system complexity, spectral efficiency, and/or performance for improved linearity.

In [6] an approach is presented which transforms the high PAPR OFDM waveform into a 0 dB PAPR constant envelope OFDM-based waveform called OFDM phase modulation (OFDM-PM). The OFDM-PM signal can be viewed as a type of digital FM whereby the modulating phase signal is a real-valued OFDM baseband waveform. Obviously, the significance of the 0 dB PAPR is that the signal can be amplified with power efficient non-linear power amplifiers. As with other PAPR reduction techniques however, the corresponding trade-offs must be determined.

This paper presents new results on the spectral properties of OFDM-PM. It is shown that spectral efficiency can be improved when using small modulation indices. Also, the OFDM-PM signal space is studied by considering the correlation properties of the signal set. The optimum demodulation performance of OFDM-PM corrupted by additive white Gaussian noise (AWGN) is compared to the performance of a nonlinear sub-optimum receiver. This receiver is shown to perform very close to optimum for small modulation indices at high signal-to-noise (SNR) ratios.

SIGNAL DESCRIPTION

The bandpass OFDM-PM signal is written as

$$s(t) = A\cos\left[2\pi f_c t + \phi(t)\right] \tag{1}$$

where A is the signal amplitude and f_c is the carrier frequency. The phase signal during the nth signaling interval $nT \leq t < (n+1)T$, where T is the signaling interval duration, can be written as

$$\phi(t) = \theta_n + 2\pi h C_N \sum_{k=1}^{N} I_{nk} q_k(t - nT) \tag{2}$$

The binary data symbols $\{I_{nk}\}$ take on values ± 1 and the phase pulses $\{q_k(t)\}$ are orthogonal OFDM subcarriers. The normalizing constant $C_N = \sqrt{2/N}$ results in a phase signal variance that is independent of the number of subcarriers N and equal to $\sigma_\phi^2 = (2\pi h)^2$, where h is the modulation index. The memory constant θ_n may be used to gain phase continuity at the signal boundaries. For memoryless modulation $\theta_n = 0$. It is noted that the

This work was supported by the UCSD Center for Wireless Communications and by the CoRe research grant 00-10071.

OFDM-PM waveform fits into the general class of digital FM signals [7], [8].

The set of subcarrier functions $\{q_k(t)\}$ satisfy the orthogonality condition

$$\int_0^T q_i(t)q_j(t)dt = \begin{cases} \mathcal{E}_{\text{sub}} & (i=j) \\ 0 & (i \neq j) \end{cases} \tag{3}$$

where $\mathcal{E}_{\text{sub}}$ is the subcarrier energy. Equation 3 is satisfied by the set of half-cosines

$$q_k(t) = \begin{cases} \cos \pi kt/T & (0 \leq t < T) \\ 0 & (\text{otherwise}) \end{cases}, \quad k = 1, \ldots, N \tag{4}$$

or the set of half-sines

$$q_k(t) = \begin{cases} \sin \pi kt/T & (0 \leq t < T) \\ 0 & (\text{otherwise}) \end{cases}, \quad k = 1, \ldots, N \tag{5}$$

In conventional OFDM the discrete Fourier transform (DFT) is used for modulation/demodulation [9]. As discussed in [6] the real-valued (or imaginary-valued) part of the OFDM baseband waveform can be used in OFDM-PM. In this case, using the notation of (2), $N/2$ full-cosines and $N/2$ full-sine waves are modulated by the N real-valued data symbols[1].

Figure 1 shows examples of the generated phase waveform $\phi(t)$ for $N = 16$ subcarriers and modulation index $h = 0.6/2\pi$. Memoryless OFDM-PM ($\theta_n = 0$) with half-cosines and half-sines is shown in Fig. 1(a) and 1(b), respectively. The half-sine case yields a phase signal which is continuous at the signaling boundaries $t = 16T_b, 32T_b, \ldots$, ($T_b = T/N$ is the bit time interval), while the half-cosine phase signal has discontinuities at the boundaries. Continuous phase is achieved by introducing memory ($\theta_n \neq 0$) as shown in Fig. 1(c).

SPECTRAL PROPERTIES

In [6] the Carson and RMS bandwidths are used to estimate the spectral requirements of OFDM-PM. For a better understanding of the spectrum other techniques are required. In [10] a general approach of evaluating the power density spectrum of digital FM signals is presented which includes the numerical evaluation of a two-dimensional integral. For common digital phase modulation formats [11] the integrand is sufficiently smooth and numerical integration algorithms converge. However, for OFDM-PM the integrand is not smooth and convergence is very difficult, especially for larger N. Alternatively, the Welch

[1]In this discussion, full-(co)sines are (co)sine waves with frequency separation $1/T$ Hz.

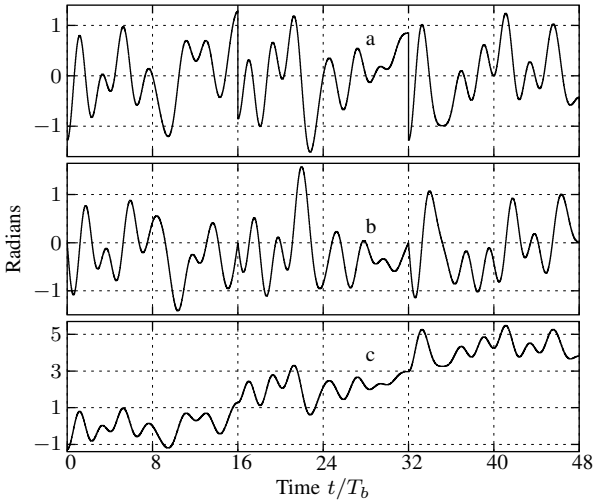

Fig. 1. Generated phase waveform $\phi(t)$ with $N = 16$ subcarriers and modulation index $h = 0.6/2\pi$ for subcarrier types: (a) half-cosine (b) half-sine and (c) half-cosine with memory.

method [12, pp. 911–913] has proven effective. This paper reports spectral estimates using Hamming windows of length 8000 with 50% overlap. The sampling rate is $F_s = 30/T_b$ and the number of averaged periodograms is 500.

Figures 2 and 3 show the power spectrum and spectral containment of the OFDM-PM signals from Fig. 1. The curves are compared to conventional OFDM with $N = 16$ subcarriers. Digital FM signals without memory are known to have spectral line components [7] and this is shown to be true for the memoryless OFDM-PM examples. With the introduction of memory, the spectral lines vanish and the spectrum is better contained.

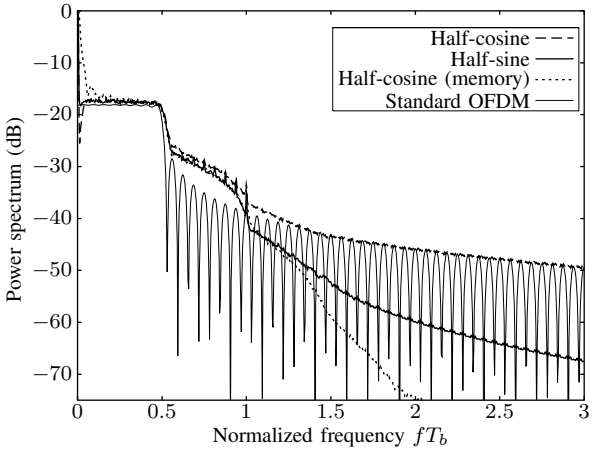

Fig. 2. Power density spectrum for OFDM-PM signals in Fig. 1 compared to standard OFDM.

The spectrum of the memoryless half-sine case is better than the spectrum of the half-cosine case. This is explained

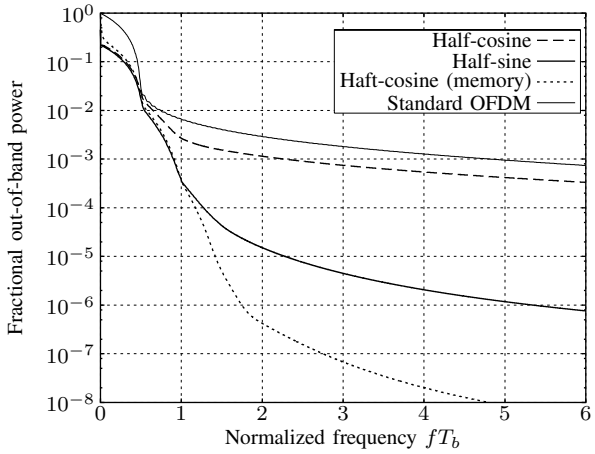

Fig. 3. Fractional out-of-band power curves.

by observing the phase signal in Fig. 1(b) to be relatively smoother than the phase signal in Fig. 1(a). In general, signals with smoother modulating phase signals result in better spectral containment (for example, see [13]).

Figure 3 shows that the fractional out-of-band power of the half-sine case is the same as the phase-continuous half-cosine signal for $fT_b \leq 1$ and a containment greater than 99.9% at $fT_b = 1$. The 99% bandwidths of the OFDM-PM signals (at $fT_b \approx 0.5$) are very similar to the standard OFDM signal[2]. Surprisingly, for the other values of fT_b the OFDM-PM signals have better containment than the conventional OFDM signal. This is not true in general since the spectral requirements for OFDM-PM increases for larger modulation index. Figure 4 shows the power containment for various h.

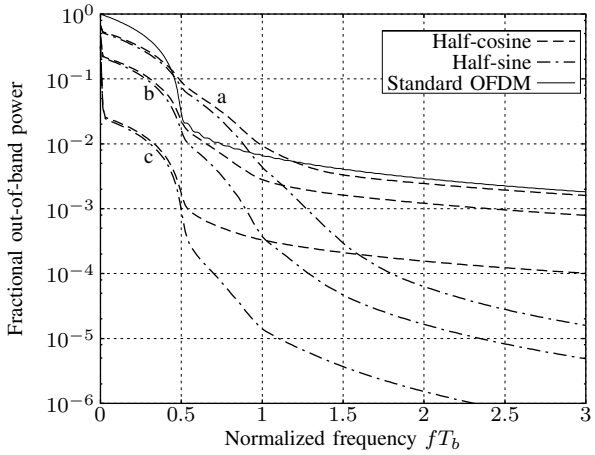

Fig. 4. Fractional out-of-band power for: (a) $h = 1/2\pi$, (b) $h = 0.6/2\pi$, and (c) $h = 0.2/2\pi$.

[2]These are single-sided bandwidths. The actual bandwidth is twice this.

SIGNAL CORRELATION

In this section the correlation among memoryless OFDM-PM signals is studied. From these correlation properties, a bound on the minimum Euclidean distance is determined.

During any signaling interval there are 2^N unique OFDM-PM transmit signals corresponding to the 2^N binary data n-tuples. During the zeroth interval, the ith OFDM-PM signal is

$$s_i(t) = A\cos\left[2\pi f_c t + K\sum_{k=1}^{N} I_{ik} q_k(t)\right] \tag{6}$$

for $0 \leq t < T$, where $K = 2\pi h C_N$. The normalized correlation coefficient, as a function of K, is

$$\begin{aligned}\rho_{ij}(K) &= \frac{1}{\mathcal{E}_s}\int_0^T s_i(t)s_j(t)dt \\ &= \frac{A^2}{2\mathcal{E}_s}\int_0^T \mathrm{Re}\left[\exp\left\{j2K\sum_{k=1}^{N}\Delta_{ij}(k)q_k(t)\right\}\right]dt \\ &= \frac{A^2}{2\mathcal{E}_s}\int_0^T \mathrm{Re}\left[\prod_{d=1}^{D}\exp\left\{j2K\Delta_{ij}(k_d)q_{k_d}(t)\right\}\right]dt\end{aligned} \tag{7}$$

where $j = \sqrt{-1}$, $\mathcal{E}_s = A^2T/2$ is the signal energy, and $\Delta_{ij}(k) = (I_{ik} - I_{jk})/2$. Notice that $\{k_d\}_{k=1}^{D}$ represent the subcarrier location where the data symbols differ, (i.e. $\Delta_{ij}(k_d) \neq 0$), and D is total number of differences. Equation 7 assumes the contribution of double frequency terms to be negligible.

It is now shown that $\rho_{ij}(K)$ can be written as a sum of Bessel function products. First, consider using the half-cosine functions in (4) for the phase pulses $\{q_k(t)\}$ and note the expansion [14]

$$e^{ja\cos b} = \sum_{n=-\infty}^{\infty} J_n(a)e^{jn(b+\pi/2)} \tag{8}$$

where $J_n(a)$ is the nth order Bessel function of the first kind. Now, (7) can be written as

$$\begin{aligned}\rho_{ij}(K) = \frac{A^2}{2\mathcal{E}_s}\int_0^T \mathrm{Re}\Bigg[&\sum_{n_1=-\infty}^{\infty}\cdots\sum_{n_D=-\infty}^{\infty} J_{n_1}(2K\Delta_{ij}(k_1))\times \\ &\cdots\times J_{n_D}(2K\Delta_{ij}(k_D))e^{j\sigma(\vec{n})}\Bigg]dt \\ = \frac{A^2}{2\mathcal{E}_s}\int_0^T &\sum_{n_1=-\infty}^{\infty}\cdots\sum_{n_D=-\infty}^{\infty} J_{n_1}(2K\Delta_{ij}(k_1))\times \\ &\cdots\times J_{n_D}(2K\Delta_{ij}(k_D))\cos[\omega(\vec{n})+\psi(\vec{n})]dt\end{aligned} \tag{9}$$

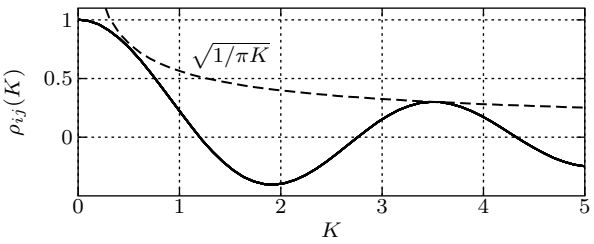

Fig. 5. Correlation for $D = 1$.

where $\sigma(\vec{n}) = \omega(\vec{n}) + \psi(\vec{n})$, $\omega(\vec{n}) = \frac{\pi t}{T} \sum_{d=1}^{D} k_d n_d$ and $\psi(\vec{n}) = \frac{\pi}{2} \sum_{d=1}^{D} n_d$. Index vectors $\vec{n}$ resulting in $\omega(\vec{n}) \neq 0$ have zero contribution thus (9) simplifies to

$$\rho_{ij}(K) = \sum_{m} \prod_{d=1}^{D} J_{\lambda_{md}}(2K\Delta_{ij}(k_d)) \cos[\psi(\vec{\lambda}_m)] \quad (10)$$

where $\vec{\lambda}_m = [\lambda_{1m}, \ldots, \lambda_{Dm}]$, $m = 1, 2, \ldots$, represent the vectors whereby $\omega(\vec{\lambda}_m) = 0$. Using half-sines for $\{q_k(t)\}$ yields the same result as (10) with $\psi(\vec{\lambda}_m) = 0$ since $e^{ja \sin b} = \sum_{n=-\infty}^{\infty} J_n(a) e^{jnb}$.

A few comments are in order for (10). First, the correlation between two OFDM-PM signals is directly dependant on the difference vector defined as $\vec{\Delta}_{ij} \equiv [\Delta_{ij}(k_1), \ldots, \Delta_{ij}(k_D)]$. Furthermore, the polarity of $\Delta_{ij}(k_d)$ affects the correlation since, depending on the order, $J_n(a)$ can be an odd or an even function. For example, signal pairs with $\vec{\Delta}_{ij} = [+1, +1, +1]$ have a different correlation than signal pairs with $\vec{\Delta}_{ij} = [+1, +1, -1]$. Therefore, the correlation is not a function of D alone. Also, the number of signal pairs is $\binom{2^N}{2}$ but since the correlation functions depend only on $\vec{\Delta}_{ij}$, there are no more than 3^N unique correlation function.

A. $D = 1$, *General* N

For $D = 1$ the correlation function simplifies to

$$\rho_{ij}(K) = J_0(2K) \quad (11)$$

and is plotted in Fig. 5. The dotted curve is the envelope of the zeroth order Bessel function [14, p. 121]. Notice that for $D = 1$, the correlation is not influenced by the number of subcarriers N or by the subcarrier location where the data symbols differ.

B. $N = 4$ *and* $N = 8$

For the $D = 1$ case, the solution simplifies to a single term. Unfortunately, for $D > 1$ the analytical solution (10) has an infinite number of terms since there are there is an unlimited number of valid index vectors $\vec{\lambda}_m$. In this case, it is easier to compute (7) numerically. Figure 6 plots

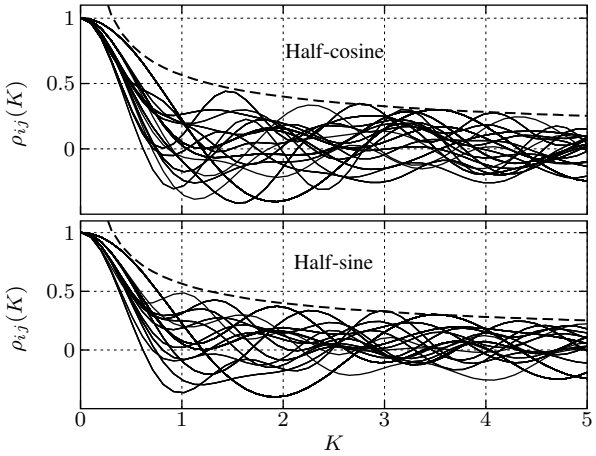

Fig. 6. Correlation functions for $N = 4$.

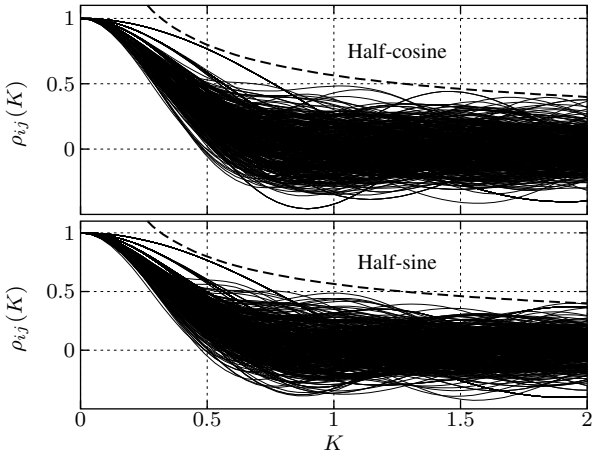

Fig. 7. Correlation functions for $N = 8$.

all the the correlation functions for $N = 4$. Notice that the half-cosine signals have a lower maximum correlation than the half-sine signals at most values of K. Figure 7 plots all the possible correlation functions for $N = 8$. For all examples, the correlation functions are bound by $\sqrt{1/\pi K}$.

OPTIMUM RECEIVER

Consider the received signal

$$r(t) = s(t) + n_w(t), \qquad 0 \leq t < T \quad (12)$$

where $n_w(t)$ is a sample function of the additive white Gaussian noise process with power spectral density $\Phi_{n_w n_w}(f) = N_0/2$ W/Hz. The optimum receiver [15, p. 244], shown in Fig. 8, correlates the received signal with each potentially transmitted signal and selects the largest result. The performance is limited by the minimum Euclidean distance of the signal space, which can be

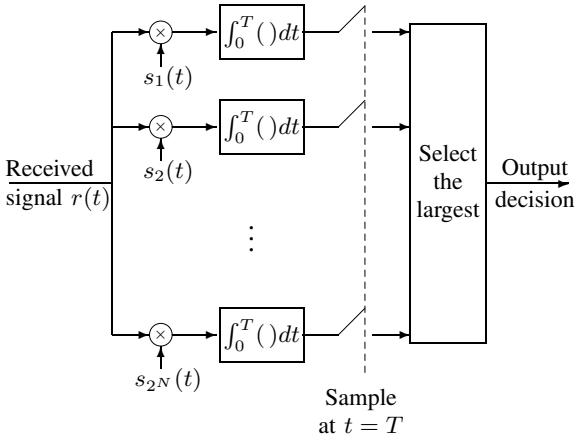

Fig. 8. Optimum receiver.

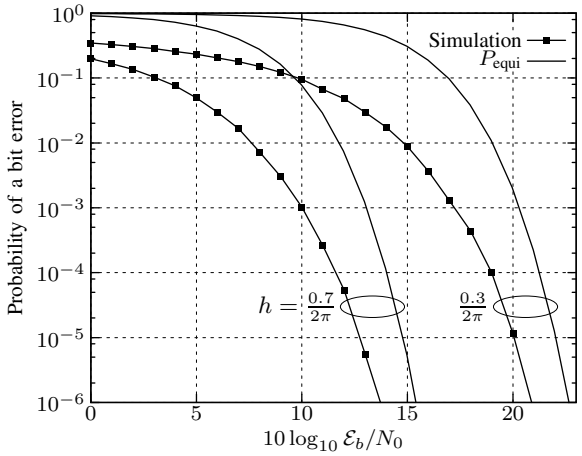

Fig. 9. Probability of a bit error for the optimum OFDM-PM receiver. ($N = 8$, half-sine subcarriers)

written as

$$d^2_{\text{min}}(K) = 2N\mathcal{E}_b[1-\rho_{\text{max}}(K)] \tag{13}$$

where $\mathcal{E}_b = \mathcal{E}_s/N$ is the energy per bit and $\rho_{\text{max}}(K)$ is the maximum signal correlation. From Fig. 6 and 7, the correlation functions are upper bounded by $\sqrt{1/\pi K}$, thus

$$d^2_{\text{min}}(K) \geq 2N\mathcal{E}_b\left\{1-\min\left[1,\sqrt{\frac{1}{\pi K}}\right]\right\} \tag{14}$$

Notice, as $K\to\infty$ the OFDM-PM signals have the same distance properties as 2^N-ary orthogonal signals.

A bound on the bit error performance of the optimum receiver can be made by finding the probability of symbol error of $M = 2^N$-ary equicorrelated signals, which is [16]

$$P_{\text{equi}}(\lambda) = \frac{1}{\sqrt{2\pi}}\int_{-\infty}^{\infty}\left[1-\left(\frac{1}{\sqrt{2\pi}}\int_{-\infty}^{y}e^{-x^2/2}dx\right)^{M-1}\right] \times\exp\left[-\frac{1}{2}\left(y-\sqrt{\frac{2\mathcal{E}_s(1-\lambda)}{N_0}}\right)^2\right]dy \tag{15}$$

where $|\lambda|\leq 1$ is the correlation of the signals. The bit error probability of OFDM-PM is therefore bounded as

$$P_{\text{b}} \leq P_{\text{sym}} \leq P_{\text{equi}}(\rho_{\text{max}}(K)) \tag{16}$$

where P_{sym} is the symbol error probability. Figure 9 compares this bound to simulation results for $N = 8$ half-sine subcarriers. The maximum correlation is $\rho_{\text{max}}(K) = 0.8811$ for $h = 0.7/2\pi$ and 0.9776 for $h = 0.3/2\pi$. At low SNR the bound is overly pessimistic, but for higher values of $\mathcal{E}_b/N_0$ the bound is within 2 dB of the simulation results.

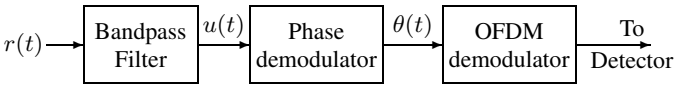

Fig. 10. A sub-optimum phase demodulator receiver.

A SUB-OPTIMUM RECEIVER

The receiver shown in Fig. 10 consists of a phase demodulator followed by a conventional OFDM demodulator. This receiver is much simpler since N matched filters are required, compared to 2^N for the optimum receiver. In this section, the performance of the PM receiver is studied.

The presence of the nonlinear phase demodulator complicates the analysis. However, for small modulation index and high SNR the problem becomes fairly linear and the bit error probability can be approximated. It is shown that under these conditions, the performance of the PM receiver is near optimum.

As is customary, the received signal $r(t)$ is assumed to be passed through an ideal bandpass filter with output

$$u(t) = s(t) + n(t) \tag{17}$$

where $n(t)$ is referred to as *bandpass white noise* [15, p. 158]. That is, the bandpass filter is sufficiently wide to pass $s(t)$ with negligible distortion while limiting the bandwidth of the additive noise signal. Consequently, $n(t)$ can be represented as

$$\begin{aligned} n(t) &= n_c(t)\cos 2\pi f_c t - n_s(t)\sin 2\pi f_c t \\ &= N(t)\cos(2\pi f_c t + \Theta(t)) \end{aligned} \tag{18}$$

where $n_c(t)$ and $n_s(t)$ are the in-phase and quadrature noise components; the noise envelope is

$$N(t) = \sqrt{n_c^2(t)+n_s^2(t)} \tag{19}$$

and the noise phase signal is

$$\Theta(t) = \arctan\left(\frac{n_s(t)}{n_c(t)}\right) \tag{20}$$

Equation 17 can now be written in the polar form

$$z(t) = R(t)\cos(2\pi f_c t + \theta(t)) \tag{21}$$

where

$$R(t) = \sqrt{[A\cos\phi(t) + n_c(t)]^2 + [A\sin\phi(t) + n_s(t)]^2} \tag{22}$$

is the received envelope,

$$\theta(t) = \arctan\left(\frac{A\sin\phi(t) + n_s(t)}{A\cos\phi(t) + n_c(t)}\right) \tag{23}$$

is the received phase signal, which can also be written as [17, p. 416]

$$\theta(t) = \phi(t) + \xi(t) \tag{24}$$

where

$$\xi(t) = \arctan\left(\frac{N(t)\sin[\Theta(t) - \phi(t)]}{A + N(t)\cos[\Theta(t) - \phi(t)]}\right) \tag{25}$$

is the noise signal. Assuming high SNR, $\xi(t)$ is approximately zero-mean Gaussian noise [18] with power density spectrum [20, p. 410]

$$\Phi_{\xi\xi}(f) \approx \frac{N_0}{A^2}, \quad |f| \le \frac{N}{2T} \tag{26}$$

for the in-band frequency range of $\phi(t)$.

The output of the ideal phase demodulator is $\theta(t)$ which is processed by the OFDM demodulator. The kth OFDM correlator computes[3]

$$\begin{aligned}\frac{1}{T}\int_0^T \theta(t)q_k(t)dt &= \frac{1}{T}\int_0^T [\phi(t) + \xi(t)]q_k(t)dt \\ &\equiv S_k + N_k\end{aligned} \tag{27}$$

where the signal component is

$$\begin{aligned}S_k &= \frac{1}{T}\int_0^T \phi(t)q_k(t)dt \\ &= \frac{2\pi h C_N}{T}\int_0^T \left(\sum_{n=1}^{N} I_n q_n(t)\right) q_k(t)dt \\ &= \frac{2\pi h C_N}{T} I_k \mathcal{E}_k \in \left\{\pm 2\pi h\sqrt{1/2N}\right\}\end{aligned} \tag{28}$$

and the noise component[4],

$$N_k = \frac{1}{T}\int_0^T \xi(t)\sin\pi k/T \tag{29}$$

[3]It is instructive to view the correlation in the continuous-time domain. For comparison, a discrete-time correlator is studied in [6].

[4]For notational simplicity, half-sine subcarriers are assumed, thus $q_k(t) = \sin\pi kt/T$. The final result is the same for half-cosines.

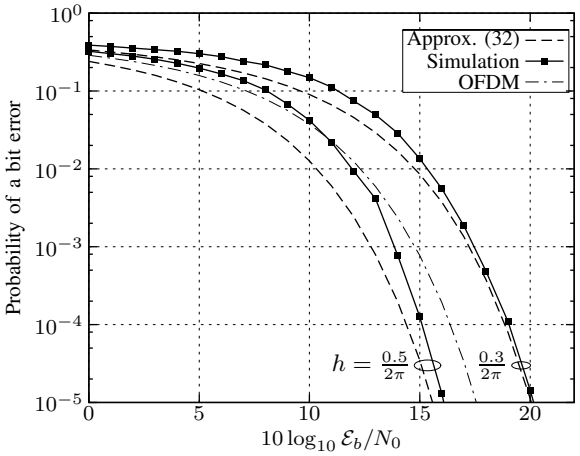

Fig. 11. Simulation results of the sub-optimum OFDM-PM receiver with $N = 16$ half-sine subcarriers. The OFDM curve accounts for an 8 dB power gain.

is approximated as a zero-mean Gaussian random variable (assuming high SNR) with variance[5]

$$E[N_k^2] \approx \frac{1}{2T}\Phi_{\xi\xi}(f)|_{f=k/2T} = \frac{1}{2T}\frac{N_0}{A^2} \tag{30}$$

The probability of a bit error for the kth demodulator is then approximated by

$$\begin{aligned}P_{k,\text{approx}} &= Q\left(\frac{|S_k|}{\sqrt{E\left[N_k^2\right]}}\right) \\ &= Q\left(2\pi h\sqrt{\frac{2\mathcal{E}_b}{N_0}}\right)\end{aligned} \tag{31}$$

Finally, since (31) is independent of k, the overall error probability is

$$P_\text{b} \approx P_{\text{b,approx}} = Q\left(2\pi h\sqrt{\frac{2\mathcal{E}_b}{N_0}}\right) \tag{32}$$

Figure 11 compares simulation results to (32) for memoryless OFDM-PM using $N = 16$ half-sine subcarriers. The sampling rate for the simulation is $F_s = 6/T_b$. The approximation is shown to be optimistic for all values of $\mathcal{E}_b/N_0$. However for $\mathcal{E}_b/N_0$ greater than 15 dB, the small modulation index example $h = 0.3/2\pi$ shows $P_{\text{b,approx}}$ to closely match the simulation result. For the large modulation index example $h = 0.5/2\pi$, the approximation is less accurate but still within 1 dB for $\mathcal{E}_b/N_0$ greater than 13 dB.

[5]This approximation is made by viewing (29) as a Fourier coefficient of $\xi(t)$ at $f_k = k/2T$ Hz. As $T \to \infty$, the variance of the coefficient is proportional to the power density spectrum (26) evaluated at $f = f_k$ (see [19, pp. 41–43]).

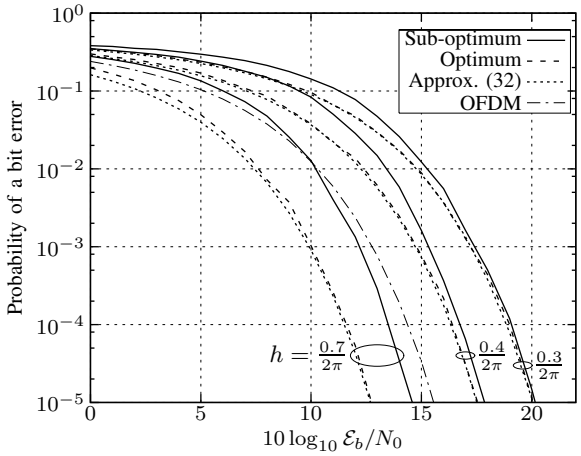

Fig. 12. Comparison of sub-optimum and optimum receiver performance ($N = 8$, half-sine subcarriers). The OFDM curve accounts for a 6 dB power gain.

Included in Fig. 11 is the performance of conventional OFDM with binary data symbols. Both system are assumed to be operating in the ideal region of the power amplifier, therefore the bit error probability of the OFDM system is $Q\left(\sqrt{2\mathcal{E}_b/N_0}\right)$. The performance curve is offset by 8 dB which accounts for an OFDM-PM power gain. In other words, the OFDM-PM system is assumed to have 8 dB less power backoff than the conventional OFDM system.

Figure 12 compares the simulation results of the optimum and sub-optimum receivers for $N = 8$ half-sine subcarriers. The conventional OFDM curve accounts for a 6 dB power gain. For the lowest modulation index example $h = 0.3/2\pi$, the sub-optimum receiver is shown to perform nearly as well as the optimum receiver for $\mathcal{E}_b/N_0 > 12$ dB. For the larger values of h, the sub-optimum receiver is shown to be increasingly worse than the optimum: ≈0.5 dB for $h = 0.4/2\pi$ and ≈2 dB for $h = 0.7/2\pi$. Interestingly, the approximation result of the sub-optimum receiver (32) is shown to match the simulation results for the optimum receiver for high SNR.

CONCLUSION

In this paper, the spectral properties of OFDM-PM are studied. It is shown that the fractional out-of-band power of OFDM-PM signals can be better than conventional OFDM. The spectrum can be further improved by introducing memory to obtain a continuous phase. The OFDM-PM signal space is studied by considering the correlation properties of the signal set and deriving a bound on the minimum Euclidean distance. The sub-optimum PM demodulator is analyzed and compared to the optimum OFDM-PM receiver. It is shown that the sub-optimum receiver performs close to optimum for a small modulation index and at high SNRs.

*

References

[1] S. Shepherd, J. Orriss, and S. Barton, "Asymptotic Limits in Peak Envelope Power Reduction by Redundant Coding in Orthogonal Frequency-Division Multiplex Modulation," *IEEE Trans. Commun.*, vol. 46, pp. 5–10, Jan. 1998.

[2] V. Tarokh and H. Jafarkhani, "On the Computation and Reduction of the Peak-to-Average Power Ratio in Multicarrier Communications," *IEEE Trans. Commun.*, vol. 48, pp. 37–44, Jan. 2000.

[3] F. H. Raab *et. al.*, "Power Amplifiers and Transmitters for RF and Microwave," *IEEE Trans. Microwave Theory Tech.*, vol. 50, pp. 814–826, Mar. 2002.

[4] P. Banelli, G. Baruffa, and S. Cacopardi, "Effects of HPA Non Linearity on Frequency Multiplexed OFDM Signals," *IEEE Trans. Broadcast.*, vol. 47, pp. 123–136, June 2001.

[5] R. van Nee and R. Prasad, *OFDM for Wireless Multimedia Communications*. Boston: Artech House, 2000.

[6] S. C. Thompson, J. G. Proakis, and J. R. Zeidler, "Binary OFDM Phase Modulation," in *Proc. of IEEE MILCOM*, (Boston), Oct. 2003.

[7] R. R. Anderson and J. Salz, "Spectra of Digital FM," *Bell Syst. Tech. J.*, vol. 44, pp. 1165–1189, 1965.

[8] J. B. Anderson, T. Aulin, and C.-E. Sundberg, *Digital Phase Modulation*. New York: Plenum Press, 1986.

[9] IEEE P802.11a/D7.0, *Supplement to Standard for Telecommunications and Information Exchange Between Systems - LAN/MAN Specific Requirements - Part 11: Wireless MAC and PHY Specifications: High Speed Physical Layer in the 5-GHz Band*, July 1999.

[10] T. Aulin and C.-E. Sundberg, "An easy way to calculate power spectra of digital FM," *IEE Proc.*, vol. 130, pp. 519–526, Oct. 1983.

[11] T. Aulin and C.-E. W. Sundberg, "Continuous Phase Modulation–Part I: Full Response Signaling," *IEEE Trans. Commun.*, vol. 29, pp. 196–209, Mar. 1981.

[12] J. G. Proakis and D. G. Manolakis, *Digital Signal Processing: Principles, Algorithms, and Applications*. Upper Saddle River, NJ: Prentice Hall, 3rd ed., 1996.

[13] F. de Jager and C. B. Dekker, "Tamed Frequency Modulation, A Novel Method to Achieve Spectrum Economy in Digital Transmission," *IEEE Trans. Commun.*, vol. 26, pp. 534–542, May 1978.

[14] E. W. Weisstein, *CRC Concise Encyclopedia of Mathematics*. Boca Raton, FL: Chapman & Hall/CRC, 2nd ed., 2003.

[15] J. G. Proakis, *Digital Communications*. New York: McGraw-Hill, 4th ed., 2001.

[16] A. H. Nuttall, "Error Probabilities for Equicorrelated M-ary Signals Under Phase-Coherent and Phase-Incoherent Reception," *IRE Trans. Inform. Theory*, pp. 305–314, July 1962.

[17] R. E. Ziemer and W. H. Tranter, *Principles of Communications – Systems, Modulation, and Noise*. New York: John Wiley & Sons, 4th ed., 1995.

[18] C. R. Cahn, "Performance of Digital Phase-Modulation Communication Systems," *IRE Trans. Commun. Sys.*, pp. 3–6, May 1959.

[19] H. E. Rowe, *Signals and Noise in Communication Systems*. Princeton, N. J.: D. Van Nostrand Company, Inc., 1965.

[20] J. G. Proakis and M. Salehi, *Communication Systems Engineering*. New Jersey: Prentice Hall, 1994.